



# Ostwald ripening with non-equilibrium vacancies

A.M. Gusak<sup>a,\*</sup>, G.V. Lutsenko<sup>a</sup>, K.N. Tu<sup>b</sup>

<sup>a</sup> Department of Theoretical Physics and Laboratory of Solid State Modeling, Cherkasy National University, 81 Shevchenko Blvd., 18027 Cherkasy, Ukraine

<sup>b</sup> Department of Materials Science and Engineering, UCLA, Los Angeles, USA

Received 19 July 2005; received in revised form 22 September 2005; accepted 28 September 2005

## Abstract

Ripening in non-dilute binary solutions is analyzed by taking into account the influence of non-equilibrium vacancies, generated by non-equal intrinsic fluxes of the components. A mathematical model has been developed for both coherent and incoherent precipitates. In the case of coherent precipitates the ripening kinetics demonstrates three stages, with the second stage characterized by a time exponent closer to 1/2 than to 1/3. The standard deviation of the particle size distribution is larger than that for a Lifshitz–Slyozov–Wagner distribution.

© 2005 Acta Materialia Inc. Published by Elsevier Ltd. All rights reserved.

**Keywords:** Diffusion; Coarsening; Vacancies; Mean-field theory

## 1. Introduction

Ostwald ripening, which is defined as the growth of large particles at the expense of small ones of a dispersed phase in a matrix, is driven by the tendency of a system to reduce the total interfacial energy. The first commonly accepted theory of ripening was developed by Lifshitz, Slyozov, and Wagner (LSW theory) [1,2]. In LSW theory, the ripening of the particles of pure component B in a dilute binary solution of AB is considered by using the mean-field approximation and steady-state solution of the diffusion equation around each particle. The LSW theory predicts that the average particle size changes with time as

$$\langle R \rangle^3 - \langle R_0 \rangle^3 = \frac{4}{9} D \alpha t, \quad (1)$$

where  $\alpha = c^{\text{eq}} 2\sigma\Omega/kT$  is the Gibbs–Thomson factor,  $D$  the diffusivity,  $\sigma$  the surface tension, and  $c^{\text{eq}}$  the equilibrium concentration at the flat interface with the new phase. Under the assumed condition that  $c_A \gg c_B$  in the parent

phase,  $D$  is treated as the diffusivity of species B in the parent phase of AB.

However, in the general case the treatment of  $D$  requires a more careful analysis. Among the most extensively studied systems are Ni-based alloys (for example, Ni–Al), in which the parent phase can be a concentrated solution (for example, of Al in Ni), or even an intermetallic phase (IMC) of  $\text{Ni}_3\text{Al}$  or NiAl; these are not dilute solutions at all. For such systems,  $D$  is usually treated as the coefficient of chemical diffusion (interdiffusion) determined from Darken's theory. The ripening kinetics may be used as a tool for determining the value of  $D$ . In [3], a corresponding method of determining the coefficient of interdiffusion was proposed.

In Darken's theory the coefficient of interdiffusion has the following form:

$$\tilde{D} = (c_A D_B^* + c_B D_A^*) \varphi, \quad (2)$$

where  $D_B^*$  and  $D_A^*$  are the self-diffusivities of species B and A, respectively, and  $\varphi$  is the thermodynamic factor. The results of Darken's theory were obtained under the assumption of local vacancy quasi-equilibrium [4]. It was assumed that the vacancy concentration is equal to its equilibrium value  $c_V^{\text{eq}}$ . However, this assumption is not always

\* Corresponding author. Tel.: +380 47 2 371220.

E-mail addresses: gusak@cdu.edu.ua, gusak@routec.net (A.M. Gusak), gala@phys.cdu.edu.ua (G.V. Lutsenko), kntu@ucla.edu (K.N. Tu).

true because Kirkendall voids have been observed in many cases of interdiffusion. The void formation is due to supersaturation of non-equilibrium vacancies in the region of the interdiffusion zone. The question arises as to whether the application of Darken's assumption to the ripening theory is always correct or not.

Considering that ripening is a very slow process, it has been suggested that non-equilibrium vacancies have time to "escape" to sinks and, therefore, the approach of local vacancy equilibrium is valid. However, the difference of the mobilities of A and B atoms should constantly generate local vacancy fluxes and, therefore, local deviations from equilibrium.

For example, if a precipitate (rich in B component) is overcritical and, hence, is growing, it means that the concentration of species B near the interface is lower than the mean-field value. Thus, in the vicinity of a precipitate the intrinsic flux of B (in the parent lattice reference frame) is directed to the particle, and the flux of A is in the opposite direction. If the mobility of B atoms is larger than that of A atoms, the intrinsic flux of B will be larger than the flux of A. This difference of intrinsic fluxes will generate the vacancy flux in the same direction as that of A (out of the particle). Therefore, the depletion of vacancies and the corresponding vacancy concentration gradient should be formed in the vicinity of the precipitate. This vacancy gradient will influence the fluxes of the main species, decreasing the larger intrinsic flux of B and increasing the smaller intrinsic flux of A. In the standard approach the vacancy sinks/sources are assumed to have absolute efficiency, providing a very fast relaxation of vacancy concentration in each point and making all deviations of vacancy concentrations from equilibrium negligible.

If the "length of the mean free path" of vacancies to sinks is comparable to interparticle distance in ripening, such deviations from equilibrium should not be neglected. If the interparticle distance is about a few tens or even hundreds of nanometers, vacancies have a good chance to migrate between precipitates without being annihilated at sinks. For larger ratios of intrinsic diffusivities ( $D_A/D_B$ ) larger deviations from equilibrium could be expected. For intermetallic phases the ratio  $D_A/D_B$  may be very different from unity. For example, in the NiAl system, the deviation of composition from the stoichiometric value leads to a sharp increase of the mobility of the majority component [5]. Consequently, the fluxes of A and B may be very different from each other and a significantly uncompensated flux of vacancies can be generated in the vicinity of each precipitate, leading to their redistribution and a change of the fluxes of the two components. In order to achieve the equilibrium vacancy concentration, an efficient network of sources and sinks is required.

To our knowledge, the first consistent treatment of interdiffusion taking into account non-equilibrium vacancies was proposed by Nazarov and Gurov [6–8]. However, they did not take into account the sinks and sources explicitly. The coefficient of interdiffusion was given as

$$D_{\text{NG}} = \frac{D_A^* D_B^* \phi}{c_A D_A^* + c_B D_B^*} \quad (3)$$

and it coincided with the well-known expression for interdiffusivity in ionic compounds (Nernst–Planck equation). Later, in [9] a more general approach was proposed, treating the system with limited efficiency of vacancy sinks/sources in a diffusion couple. It was demonstrated that the very initial stage of interdiffusion is governed by an effective diffusivity according to Eq. (3) (controlled by the slow species). At a late stage it is governed by Darken's interdiffusivity, and at an intermediate stage (for annealing time  $t \sim \tau_V/c_V$ , where  $\tau_V$  is the vacancy relaxation time and  $c_V$  the vacancy concentration) diffusion is non-parabolic and even non-local.

In the following, we apply the ideas mentioned above to ripening in non-dilute solutions. Namely, we treat the ripening in a system where a mass transfer is controlled by interdiffusion with significantly different mobilities of species and with limited vacancy sink/source efficiency.

## 2. Ripening kinetics with non-equilibrium vacancies

Consider the ripening of a set of spherical particles with equilibrium concentration  $c_B^\gamma$  (phase  $\gamma$ ) in a solid solution of AB (phase  $\alpha$ ). The balance equation for the flux  $J_B$  of B at the interphase boundary of  $R$  is

$$n_\alpha(-J_B)4\pi R^2 dt = (n_\gamma c_B^\gamma - n_\alpha c_B^\alpha)4\pi R^2 dR. \quad (4)$$

Assuming  $n_\alpha = n_\gamma$ , we obtain

$$\frac{dR}{dt} = -\frac{J_B(R)}{c_B^\gamma - c_B^\alpha}. \quad (5)$$

As is shown in Appendix A, the fluxes of A and B and vacancies in the laboratory reference frame taking into account non-equilibrium vacancies (but without Manning's corrections) are the following [9]:

$$\begin{cases} \Omega J_A = \tilde{D} \nabla c_B - (D_B^* - D_A^*) \frac{c_A c_B}{c_V} \nabla c_V, \\ \Omega J_B = -\tilde{D} \nabla c_B + (D_B^* - D_A^*) \frac{c_A c_B}{c_V} \nabla c_V, \\ \Omega J_V = (D_B^* - D_A^*) \phi \nabla c_B - D_V \nabla c_V. \end{cases} \quad (6)$$

(Of course, in a laboratory reference frame the fluxes of A and B are equal in magnitude, as it should be due to the conservation of matter.)

Thus, the redistribution of atoms and vacancies in such a system can be described by the following set of equations:

$$\begin{cases} \frac{\partial c_B}{\partial t} = \tilde{D} \nabla^2 c_B - (D_B^* - D_A^*) \frac{c_A c_B}{c_V} \nabla^2 c_V, \\ \frac{\partial c_V}{\partial t} = -(D_B^* - D_A^*) \phi \nabla^2 c_B + D_V \nabla^2 c_V - \frac{c_V - c_V^{\text{eq}}}{\tau_V}. \end{cases} \quad (7)$$

Here, we consider only the last stage of ripening when all concentrations in the parent phase are close to equilibrium values. Then all concentration gradients are small, and we can linearize Fick's second law by taking the diffusivities out of spatial derivatives and treating them as constants.

Since ripening is a slower process than the diffusion between precipitates, we can use the standard steady-state approximation ( $\partial c_B/\partial t \approx 0$ ,  $\partial c_V/\partial t \approx 0$ ) for B and vacancies. Then:

$$\begin{cases} \tilde{D}\nabla^2 c_B - (D_B^* - D_A^*) \frac{c_A c_B}{c_V} \nabla^2 c_V = 0, \\ -(D_B^* - D_A^*) \varphi \nabla^2 c_B + D_V \nabla^2 c_V - \frac{c_V - c_V^{\text{eq}}}{\tau_V} = 0. \end{cases} \quad (8)$$

Using some simple algebra, we obtain from Eq. (8)

$$\nabla^2 (c_V - c_V^{\text{eq}}) = \frac{1}{\lambda^2} (c_V - c_V^{\text{eq}}) \quad (9)$$

with

$$\lambda^2 = L_V^2 \frac{D_{\text{NG}}}{\tilde{D}}, \quad (10)$$

where  $L_V = \sqrt{\tau_V D_V}$  is the length of the mean free path of vacancies and  $D_{\text{NG}}$  is the interdiffusivity for the system with zero efficiency of vacancy sinks ( $L_V \rightarrow \infty$ ), as given by Eq. (3).

Eq. (9) represents a screening-type equation. Its standard solution in the spherically symmetrical case has the following form:

$$\hat{c}_V \equiv c_V - c_V^{\text{eq}} = \frac{A}{r} e^{-r/\lambda} \quad (11)$$

and  $\lambda$  has the meaning of a screening length, which is related to the efficiency of sinks and sources of vacancies.

Using Eqs. (11) and (8), we obtain the expressions for  $\nabla^2 c_B$ ,  $\nabla c_B$ , and  $c_B$ :

$$\frac{\partial}{\partial r} \left( r^2 \frac{\partial c_B}{\partial r} \right) = A \frac{(D_B^* - D_A^*)}{\lambda^2 \tilde{D}} \frac{c_A c_B}{c_V} r e^{-r/\lambda}, \quad (12)$$

$$\frac{\partial c_B}{\partial r} = \frac{1}{r^2} \left( K_1 - A \frac{(D_B^* - D_A^*)}{\lambda^2 \tilde{D}} \frac{c_A c_B}{c_V} \lambda^2 \left( 1 + \frac{r}{\lambda} \right) e^{-r/\lambda} \right), \quad (13)$$

$$c_B = -\frac{K_1}{r} + K_2 + A \frac{(D_B^* - D_A^*)}{\tilde{D}} \frac{c_A c_B}{c_V} \frac{1}{r} e^{-r/\lambda}. \quad (14)$$

The three unknown parameters  $A$ ,  $K_1$ , and  $K_2$  can be determined from three boundary conditions. Two of the conditions are introduced by analogy with the LSW theory:

- (1) The concentration of B at a long distance from a particle (mean-field approximation) is given as

$$c(r \gg R) = \bar{c}. \quad (15)$$

- (2) The Gibbs–Thomson equation for the equilibrium concentration of B at the interphase boundary yields

$$c_B^{\text{eq}}(R) = c_B^{\text{eq}} + \frac{\alpha}{R}, \quad (16)$$

where  $c_B^{\text{eq}}$  is the equilibrium concentration for a flat interface.

A third condition can vary, depending on the interface structure. As a first possibility, we consider zero vacancy flux at the interface:

$$J_V|_R = 0 \quad (17)$$

and frozen lattice diffusion inside the precipitate. This corresponds to the case of coherent precipitates without effective sinks and sources, so vacancies are just reflected back into the parent phase.

The second possibility is assuming local vacancy equilibrium at curved interfaces, satisfying the Gibbs–Thomson relation for vacancies. A short analysis of such a case is presented in Appendix B.

Substituting the values obtained for  $A$ ,  $K_1$ , and  $K_2$  into Eq. (6) and using Eq. (5), we obtain the following rate of particle growth or shrinkage:

$$\frac{dR}{dt} = \frac{\Delta - \frac{\alpha}{R}}{(c_B^{\text{eq}} - c_B^{\text{eq}})R} \cdot \frac{D_{\text{NG}}(1 + \frac{R}{\lambda})}{1 + \frac{D_{\text{NG}}}{\tilde{D}} \frac{R}{\lambda}}, \quad (18)$$

where  $\Delta = \bar{c} - c_B^{\text{eq}}$  is the supersaturation.

We introduce the following special abbreviation:

$$D^{\text{ef}} = \frac{D_{\text{NG}}(1 + \frac{R}{\lambda})}{1 + \frac{D_{\text{NG}}}{\tilde{D}} \frac{R}{\lambda}}. \quad (19)$$

With this notation, Eq. (18) is very similar to the rate equation in the LSW theory, but with the effective diffusivity depending on particle size; if  $\lambda \gg R$ , then  $D^{\text{ef}}$  tends to be  $D_{\text{NG}}$  (growth controlled by the slow species), and if  $\lambda \ll R$ ,  $D^{\text{ef}}$  tends to be Darken's value of  $\tilde{D}$  (growth controlled by the fast species).

Analysis of effective diffusivities shows that one might expect a special regime of ripening in the following interval of average sizes:

$$1 \ll \frac{\langle R \rangle}{\lambda} \ll \frac{\tilde{D}}{D_{\text{NG}}} \left( \text{or } \sqrt{\frac{D_{\text{NG}}}{\tilde{D}}} \ll \frac{\langle R \rangle}{L_V} \ll \sqrt{\frac{\tilde{D}}{D_{\text{NG}}}} \right). \quad (20)$$

These conditions correspond to a large ratio of  $\tilde{D}/D_{\text{NG}}$ . Under this condition one can easily see that for precipitates with sizes not very far from the average one, the effective diffusivity is proportional to the particle radius, i.e.

$$D^{\text{ef}} = \frac{D_{\text{NG}}(1 + \frac{R}{\lambda})}{1 + \frac{D_{\text{NG}}}{\tilde{D}} \frac{R}{\lambda}} \approx D_{\text{NG}} \cdot \frac{R}{\lambda}. \quad (21)$$

In this case, the growth/shrinkage equation becomes similar to Hillert's equation for grain growth yielding the parabolic growth law instead of the 1/3-power law:

$$\frac{dR}{dt} = \frac{D_{\text{NG}}}{\lambda} \frac{\Delta - \frac{\alpha}{R}}{(c_B^{\text{eq}} - c_B^{\text{eq}})}, \quad \langle R \rangle \sim t^{1/2}. \quad (22)$$

At an initial stage, with a small average particle size,  $\langle R \rangle < \langle R_1 \rangle = L_V(D_{\text{NG}}/\tilde{D})^{1/2}$ , one might expect LSW-type ripening, but with a rate determined by  $D_{\text{NG}}$  (controlled by slow species) instead of Darken's interdiffusivity. At the last stage, when  $\langle R \rangle \gg \langle R_2 \rangle = L_V(\tilde{D}/D_{\text{NG}})^{1/2}$  the LSW regime should be realized again, with a rate now being determined by Darken's interdiffusivity (controlled by the fast species). Of course, these analytical considerations show only the trends, since, for example, at  $\langle R \rangle$  satisfying inequality (20), small precipitates with  $R \leq \lambda$  may exist.

3. Results and discussion

The main characteristics of ripening kinetics were investigated using computer simulations. In our model for an array of precipitates we calculated a time behavior of sizes by solving a set of differential equations (Eq. (18)) for growth/shrinkage of each particle. This equation was written and solved for cubed size instead of linear size just to escape zero in the denominator, when a particle is disappearing:

$$\frac{dR^3[i]}{dt} = 3 \frac{R[i]\Delta - \alpha}{(c_B^\gamma - c_B^\alpha)} \cdot \frac{D_{NG} \left(1 + \frac{R[i]}{\lambda}\right)}{1 + \frac{D_{NG}}{D} \frac{R[i]}{\lambda}}, \quad i = \overline{1, \dots, N}. \quad (23)$$

Also, the phase volume conservation condition (at asymptotic stage)

$$\sum_{i=1}^N \frac{dR^3[i]}{dt} = 0 \quad (24)$$

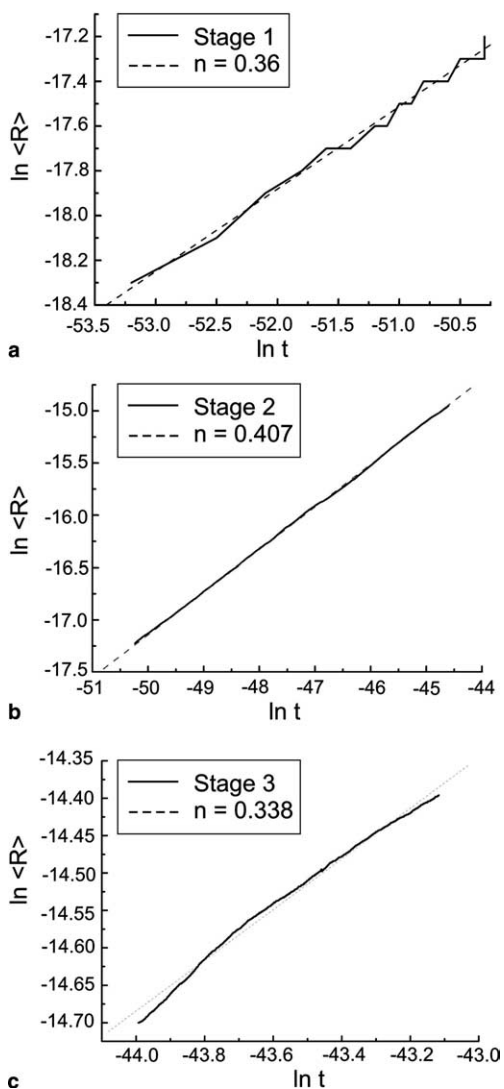


Fig. 1. Time dependence of the average radius  $\langle R \rangle$  (in logarithmic scale). (a) Stage 1, (b) Stage 2, (c) Stage 3.

was applied to calculate the supersaturation  $\Delta$  at each time step.

For convenience we used the reduced time variable:  $t = 3D_{NG}\alpha t$ . Sizes were taken in meters. Also a parameter  $\varepsilon \equiv D_{NG}/\tilde{D}$  was introduced. Evidently, if  $\varepsilon = 1$ , then Eq. (18) transforms to the LSW equation for the cubed radius. However, typically the value of  $\varepsilon$  in concentrated solutions or ordered phases can be about 0.1 or even less. The initial average size was taken as  $(1/10)L_V$  (we took  $L_{xV} = 1e - 7m$ ). We used two types of initial size distributions. In the first case it was just a uniform random

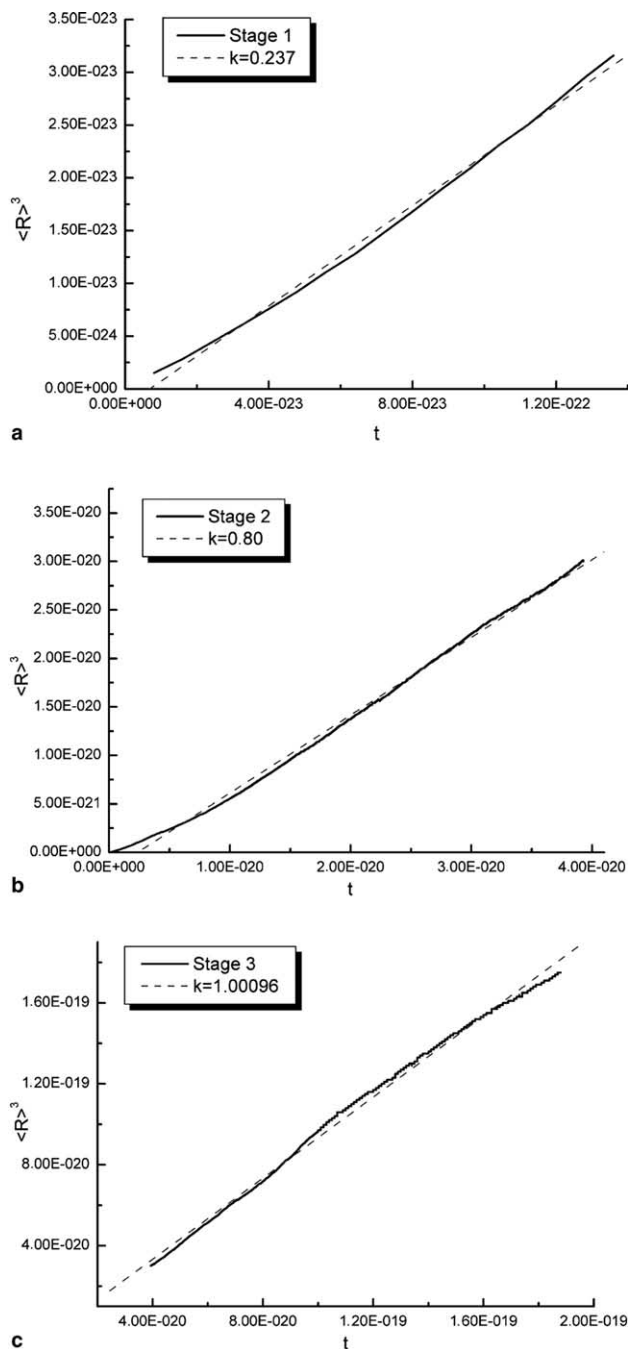


Fig. 2. Time dependence of  $\langle R \rangle^3$ . (a) Stage 1, (b) Stage 2, (c) Stage 3.

distribution within the size interval  $(0.75\langle R_0 \rangle, 1.25\langle R_0 \rangle)$ . In the second case it was the LSW distribution. At least at stages two and three the ripening kinetics was identical for both types of initial conditions. Below we present the results for the initial LSW distribution. The time dependence of the average radius  $\langle R \rangle$  (on a logarithmic scale) is shown in Fig. 1(a)–(c). Each plot was fitted to the linear dependence  $\ln \langle R \rangle = n \ln t + \text{const}$ .

In Fig. 2, the time dependence of cubed average size was plotted separately for the three stages. In the first stage ( $\langle R \rangle^3 < \langle R_1 \rangle^3 = L_V^3 (D_{NG}/\tilde{D})^{3/2}$ ), the best fit is given by a linear time dependence of the cubed mean size  $\langle R \rangle^3 = kt + \text{const}$  (Fig. 2(a)).

At the intermediate (second) stage (Fig. 2(b);  $\langle R_1 \rangle^3 = L_V^3 (D_{NG}/\tilde{D})^{3/2} \ll \langle R \rangle^3 \ll \langle R_2 \rangle^3 = L_V^3 (\tilde{D}/D_{NG})^{3/2}$ ) better agreement is obtained by a linear time dependence of the squared mean size (Fig. 3). At the last stage (Fig. 2(c)) we again observe the linear time dependence of the cubed mean size, but the rate is about 4.5 times larger than in the first stage. These results agree with the analytic approximations mentioned above. Namely, the first stage of ripening satisfies the 1/3 power-law but is controlled by the slow species. The second stage is characterized by an exponent of  $n \approx 0.4$ , which lies between the LSW ( $n = 1/3$ ) and Hillert's ( $n = 1/2$ ) values. The third stage is again of the LSW type but now it is determined by the fast species and corresponds to Ardell's analysis [10]. Realistic experiments may last too long to reach the third stage.

In addition, we plotted the particle size distributions (Fig. 4) for each stage. At the second stage our histograms are shown to be somewhere between the LSW and Hillert's distributions. The particle size distributions obtained were analyzed by introducing special parameters, which characterize width, slope, and sharpness of the peak: namely the standard deviation  $s = ((u - 1)^2)^{1/2}$ , skewness defined as  $((u - 1)^3)/s^3$ , and Kurtosis  $K = ((u - 1)^4)/s^4 - 3$ . The dependence of parameter  $s$  on  $\bar{R}$  is shown in Fig. 5. Table 1 gives the generalized data for the particle size distribution obtained and the LSW distribution.

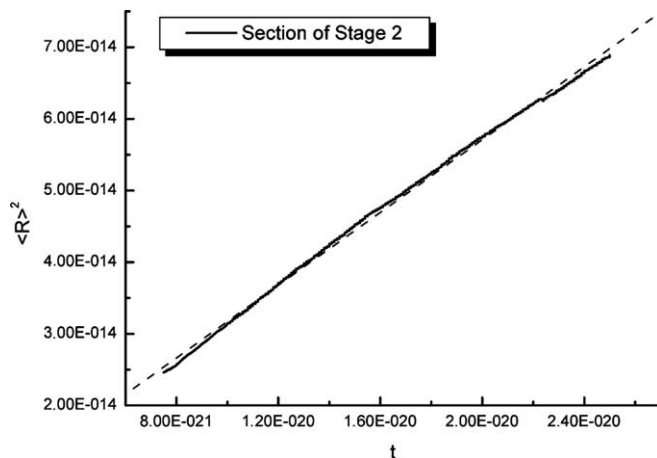


Fig. 3. Time dependence of  $\langle R \rangle^2$  for Stage 2.

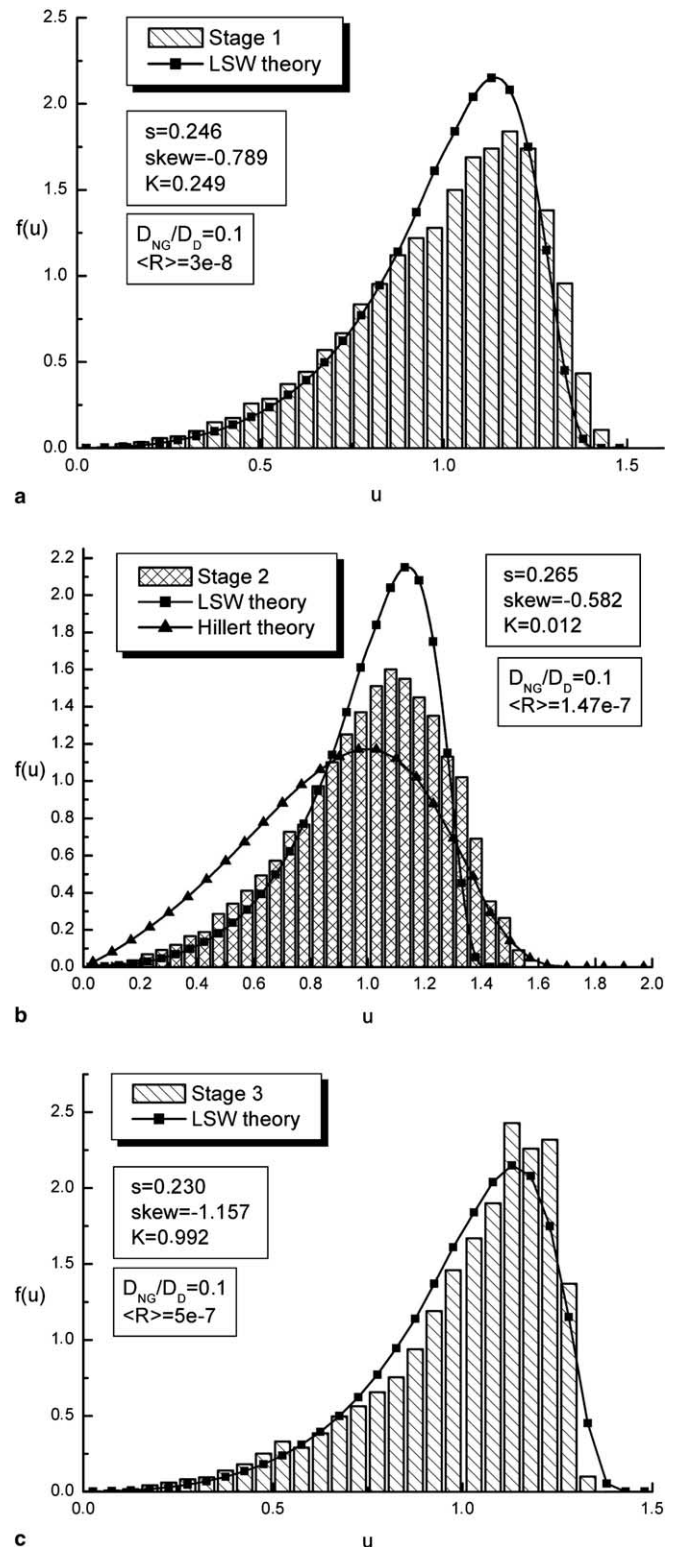


Fig. 4. Scaled particle size distribution  $f(u)$ ,  $u = R/\langle R \rangle$ . (a) Stage 1, (b) Stage 2, (c) Stage 3.

#### 4. Summary

The generation and relaxation of non-equilibrium vacancies and their spatial distribution during ripening of concentrated alloys may be important if:

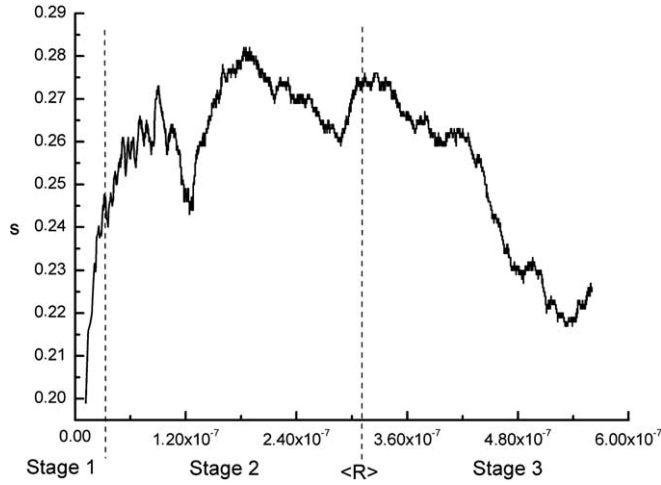


Fig. 5. Dependence of the standard deviation  $s$  on average size  $\langle R \rangle$ .

Table 1

Values of the time exponent  $n$  and typical standard deviations  $s$  for the calculated particle size distribution at each of the three stages as well as for the LSW distribution

	$n$	$S$
Stage 1	0.36	0.246
Stage 2	0.407	0.265
Stage 3	0.34	0.230
LSW	1/3	0.215

- 1) there is a significant difference between the mobilities of the alloying additions,
- 2) the distance between precipitates is comparable to the vacancy migration path,
- 3) the size of precipitates is within the interval defined by Eq. (20).

Redistribution of vacancies around precipitates inhibits the ripening rate at the “initial” stage and changes the time exponent of ripening at the intermediate stage. It also leads to a widening of the particle size distribution.

### Acknowledgements

The authors acknowledge the support by CRDF (#UE1-2523-CK-09) and the Ministry of Education and Science of Ukraine. The authors also acknowledge fruitful discussions with Dr. A.V. Nazarov, who was the first to consider the role of non-equilibrium vacancies in ripening.

### Appendix A. Interdiffusion in a system with limited vacancy sink efficiency

Consider the binary system AB (non-dilute solution B in A) in which there is a non-equilibrium spatial distribution of vacancies which builds up an additional driving force. Then the fluxes of the species A and B and the vacancy flux in the moving reference frame are obtained as:

$$\begin{cases} \Omega j_A = -L_{AA} \nabla \mu_A - L_{VA} \nabla \mu_V, \\ \Omega j_B = -L_{BB} \nabla \mu_B - L_{VB} \nabla \mu_V, \\ \Omega j_V = -L_{VV} \nabla \mu_V - L_{AV} \nabla \mu_A - L_{BV} \nabla \mu_B. \end{cases} \quad (\text{A.1})$$

The sum of the fluxes is equal to zero:

$$\sum_i j_i = 0. \quad (\text{A.2})$$

Using Eq. (A.2), we obtain:

$$\begin{cases} \Omega j_A = -L_A (\nabla \mu_A - \nabla \mu_V), \\ \Omega j_B = -L_B (\nabla \mu_B - \nabla \mu_V), \\ \Omega j_V = L_A (\nabla \mu_A - \nabla \mu_V) + L_B (\nabla \mu_B - \nabla \mu_V), \end{cases} \quad (\text{A.3})$$

where

$$L_A = \frac{c_A D_A^*}{kT}, \quad L_B = \frac{c_B D_B^*}{kT}$$

are Onsager coefficients. (Here we neglect Manning’s corrections.)

The Gibbs–Duhem relation for our system implies

$$c_A \nabla \mu_A + c_B \nabla \mu_B + c_V \nabla \mu_V = 0. \quad (\text{A.4})$$

Assuming that  $c_V \ll c_A, c_B$ , we find that

$$\nabla \mu_A = -\frac{c_B}{c_A} \nabla \mu_B. \quad (\text{A.5})$$

Then

$$\nabla (\mu_B - \mu_A) = \nabla \mu_B - \nabla \mu_A = \frac{1}{c_A} \nabla \mu_B. \quad (\text{A.6})$$

For the binary system

$$\mu_B - \mu_A = \frac{\partial g}{\partial c_B}, \quad (\text{A.7})$$

where  $g$  is the Gibbs free energy per atom.

Substituting Eq. (A.7) in Eq. (A.6), we have

$$\nabla \mu_B = c_A \nabla \left( \frac{\partial g}{\partial c_B} \right) = c_A \frac{\partial^2 g}{\partial c_B^2} \nabla c_B. \quad (\text{A.8})$$

For vacancies, we have assumed:

$$\mu_V = kT \ln(c_V/c_V^{\text{eq}}) \quad (\text{A.9})$$

and

$$\nabla \mu_V = \frac{kT}{c_V} \nabla c_V. \quad (\text{A.10})$$

Using Eqs. (A.8) and (A.10), we can find the relation for the fluxes in a moving reference frame:

$$\begin{cases} \Omega j_A = D_A^* \frac{c_A c_B}{kT} g'' \nabla c_B + D_{AV}^* \nabla c_V, \\ \Omega j_B = -D_B^* \frac{c_A c_B}{kT} g'' \nabla c_B + D_{BV}^* \nabla c_V, \\ \Omega j_V = -(j_A + j_B) = -\left( -(D_B^* - D_A^*) \frac{c_A c_B}{kT} g'' \nabla c_B + \frac{c_A D_A^* + c_B D_B^*}{c_V} \nabla c_V \right). \end{cases} \quad (\text{A.11})$$

Here,  $g'' = \partial^2 g / \partial c_B^2$ . In the laboratory reference frame, the fluxes of species are written as follows:

$$\Omega J_i = \Omega j_i + c_i u, \quad (\text{A.12})$$

where  $u$  is the Kirkendall velocity, and

$$u = \Omega j_V.$$

Using Eqs. (A.11) and (A.12) and neglecting  $c_V u$  in the expression for the vacancy flux (since  $c_V \ll 1$ ), we obtain:

$$\begin{cases} \Omega J_A = \tilde{D} \nabla c_B - (D_B^* - D_A^*) \frac{c_A c_B}{c_V} \nabla c_V, \\ \Omega J_B = -\tilde{D} \nabla c_B + (D_B^* - D_A^*) \frac{c_A c_B}{c_V} \nabla c_V, \\ \Omega J_V = (D_B^* - D_A^*) \varphi \nabla c_B - D_V \nabla c_V, \end{cases} \quad (\text{A.13})$$

where

$$\varphi = \frac{c_A c_B}{kT} g''$$

is the thermodynamics factor,  $\tilde{D} = (c_A D_B^* + c_B D_A^*) \varphi$  is Darken's interdiffusivity, and

$$D_V = \frac{c_A D_A^* + c_B D_B^*}{c_V}$$

is the vacancy diffusivity.

## Appendix B

In the case of incoherent precipitates for which local vacancy equilibrium is achieved at their curved interface, the Gibbs–Thomson relation for vacancies yields:

$$c_V^{\text{eq}}(R) = c_V^{\text{eq}} + \frac{\alpha_V}{R}, \quad (\text{B.1})$$

where  $c_V^{\text{eq}}$  is the equilibrium vacancy concentration at the flat interface, and  $\alpha_V$  is the analogue of the Gibbs–Thomson factor for vacancies.

In such a case, after simple but long algebraic calculations, determining the constants  $A$ ,  $K_1$ , and  $K_2$ , we obtain the following growth/shrinkage rate:

$$\frac{dR}{dt} = \tilde{D} \frac{A - \frac{\alpha^{\text{ef}}}{R}}{R}, \quad (\text{B.2})$$

where

$$\alpha^{\text{ef}} = \alpha - \alpha_V \frac{D_B^* - D_A^*}{\tilde{D}} \frac{c_A c_B}{c_V}.$$

The form of Eq. (B.2) corresponds to the result of LSW theory with a rescaled Gibbs–Thomson factor  $\alpha^{\text{ef}}$ . The power dependence  $\bar{R} \sim t^{1/3}$  remains, but the rate of growth varies.

## References

- [1] Lifshitz JM, Slyozov VV. J Phys Chem Solids 1961;19:35.
- [2] Wagner C. Zs Electrochem 1961;65:581.
- [3] Kim DM, Ardell AJ. Acta Mater 2003;51:4073.
- [4] Bardeen J. Phys Rev 1949;1:1403.
- [5] Gusak AM, Lyashenko YuA. Fizika Metallov Metallovedenie 1989;68:481.
- [6] Nazarov AV, Gurov KP. Fizika Metallov Metallovedenie 1974;7:496.
- [7] Nazarov AV, Gurov KP. Fizika Metallov Metallovedenie 1974;38:689.
- [8] Nazarov AV, Gurov KP. Fizika Metallov Metallovedenie 1978;45:885.
- [9] Gurov KP, Gusak AM. Fizika Metallov Metallovedenie 1985;59:1062.
- [10] Ardell AJ. In: Lorimer GW, editor. Phase transformations'87. London: Institute of Metals; 1988. p. 485.